ON THE ELECTROREDUCTION MECHANISM OF HALOBENZENES: THE SPECIAL CASE OF 1,2-DIBROMOBENZENE

Juan CASADO*, Manuel ORTEGA and Iluminada GALLARDO

Departamento de Quimica, Universidad Autonoma de Barcelona, Bellaterra, Barcelona, Spain

Received March 29, 1988
Accepted August 19, 1988

Reinvestigation of the electrochemical reduction of 1,2-dibromobenzene by polarography, cyclic voltammetry, rotating ring-disk electrode voltammetry and controlled potential electrolysis, as well as theoretical calculations, leads to the proposal of a stepwise mechanism. Experimental results for bromobenzene and 1,3-dibromobenzene are also reported for comparison.

Dihalobenzenes present in general two reduction waves corresponding to stepwise replacement of halogens by hydrogen. Nevertheless 1,2-dibromobenzene (*I*) exhibits a unique behaviour among them: it shows a single irreversible reduction wave whose $E_{1/2}$ is c. 0·55 V less negative than $E_{1/2}$ of bromobenzene. This difference has been quoted by Rifi[1] as evidence for a concerted (synchronous) abstraction of both bromides, similar to the mechanism proposed for electrochemical reduction of

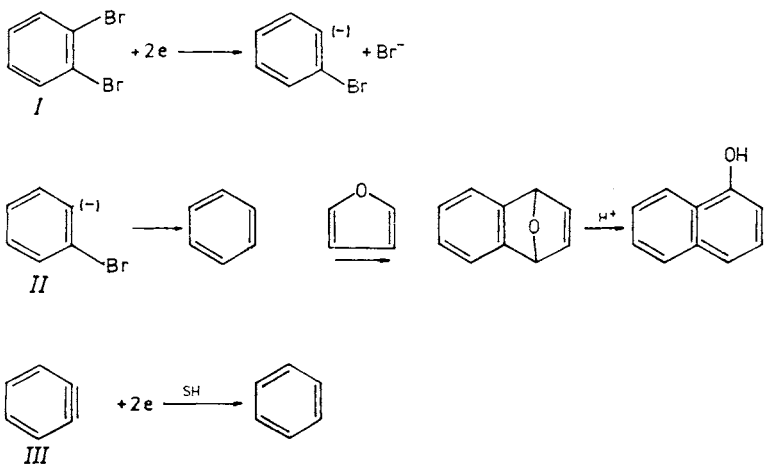

SCHEME 1

* To whom correspondence should be adressed.

aliphatic vicinal dihalides[2-4]. On the other hand, Wawzonek and Wagenknecht, the first authors who studied this reduction[5], proposed the following stepwise pathway:

Both mechanisms involve benzyne (*III*) as an intermediate. According to Wawzonek and Wagenknecht, *III* can be trapped with furane, leading, upon hydrolysis, to a small amount of 1-naphtol[5].

In 1982 Barba et al. claimed an ionic stepwise mechanism for halo and 1,2-dihalobenzenes[6], but they did not use 1,2-dibromobenzene in their work.

Therefore, feeling that the reduction mechanism of *I* remained unclear, we have tried its reinvestigation.

EXPERIMENTAL

Apparatus and techniques have been described before[7-9]. DMF purification has also been described[10]. 1,2- and 1,3-dibromobenzene (Fluka, purum) were tested by GC and were used as received. Tetraethylammonium perchlorate (TEAP) was dried under vacuum at 60°C for 24 hours. All the potentials are corrected for ohmic drop and are referred to an Ag/AgI electrode[10]. The electrolysis cell was of divided H-type with a stirred Hg pool cathode (area c. 20 cm^2) and a graphite anode. Working temperature was 25°C, unless otherwise noted.

Theoretical calculations were carried out using an MNDO semi-empirical method which was described in previous paper[7].

RESULTS AND DISCUSSION

Results of reduction of *I* by several techniques are given in Tables I–III. The first statement we can draw from these results is that bromobenzene is not formed since

TABLE I

Polarographic results of 1,2-dibromobenzene reduction compared with those for bromobenzene and 1,3-dibromobenzene in DMF/0·1M TEAP. Hg height 35 cm, m 1·3 mg s^{-1}, c 0·5 mmol l^{-1}

Compound	PhOH mmol l^{-1}	$-E_{1/2}$ V	i_l μA	I_d[c]	αn
BrC_6H_5	—	1·87	3·3	4·4	0·43
BrC_6H_5	5	1·89	4·2	5·3	0·34
1,2-$Br_2C_6H_4$	—	1·32	5·4	8·3	—[a]
1,2-$Br_2C_6H_4$	5	1·32	6·8	10·5	—[a]
1,3-$Br_2C_6H_4$	—	1·45	3·3	4·8	0·40
1,3-$Br_2C_6H_4$	5	1·44	3·8	5·5	0·34
1,3-$Br_2C_6H_4$[b]	—	1·84	2·0	3·4	0·44
1,3-$Br_2C_6H_4$[b]	5	1·82	2·5	4·2	0·47

[a] Not determined due to a maximum; [b] second wave; [c] $I_d = i_l/c \cdot m^{2/3} t^{1/6}$.

its reduction wave is not observed, neither in aprotic medium nor in presence of phenol (Tables I and II). The contrary is true for 1,3-dibromobenzene. This would imply, if one assumes the mechanism in Scheme 1, that elimination of the second bromide must be very fast in order to avoid protonation of *II* yielding bromobenzene.

The limiting diffusion current I_d of *I* is close to the sum of I_d for both waves of 1,3-dibromobenzene and almost twice the value of I_d for bromobenzene (Table I). This is also true as regards peak currents I_p in cyclic voltammetry (CV) (Table II). Therefore, it seems to be a 4-electron wave, since reduction waves of single C—Br bonds involve 2 electrons.

TABLE II

Cyclic voltammetry results of 1,2-dibromobenzene reduction compared with those for 1,3-dibromobenzene in DMF/0·1M TEAP. Cathode area 0·126 cm^2, c 1·0 mmol l^{-1}, 25·0°C

Compound	$-E_p$[a] V	$-E_{p/2}$[a] V	$dE/d \log v$[c] mV	i_p[a] μA	$i_p/v^{1/2b}$	$i_p/v^{1/2a}$	αn
1,2-$Br_2C_6H_4$	1·338	1·224	44 (0·996)	140	10·5	9·8	0·42
1,3-$Br_2C_6H_4$	1·580	1·440	53 (0·997)	85	6·9	6·0	0·36
1,3-$Br_2C_6H_4$[d]	1·942	—[e]	52 (0·992)	59	4·9	4·2	—[e]

[a] Sweep rate 200 mV s^{-1}; [b] sweep rate 20 mV s^{-1}; [c] correlation coefficients are given between parentheses; [d] second peak; [e] undetermined because of interference of the first peak.

TABLE III

Results of reduction of 1·0 mM 1,2-dibromobenzene in DMF 0·1M TEAP at the RRDE. Disk area 0·126 cm^2, E_R = 0 V vs Ag/AgI, 25·0°C

ω (rpm)	$-E_{1/2}$ V	i_D μA	i_R μA	$N_k \cdot 10^3$
70	1·232	85	1·5	18
170	1·255	130	2·9	22
500	1·290	230	5·0	22
1 000	1·297	330	6·5	20
2 000	1·317	460	7·8	17
4 000	1·342	650	9·0	14
6 000	1·353	800	9·8	12
8 000	1·361	905	—	—
10 000	1·359	975	—	—

Transfer coefficients reported in Tables I and II, around 0·4, are consistent with the values previously obtained for bromobenzene[9] and indicate that $E_{1/2} < E^0$ for the redox couples involved[11]. Transfer coefficients of *I* from RDE experiments are also in close agreement: 0·41 from Tomes criteria (averaged for all rotation speeds) and 0·47 from $E_{1/2}$ vs ln ω (correlation coefficient 0·998).

Trying to trap anion *II* we have carried out the electrolysis of *I* in presence of CO_2 at 20°C. After preelectrolysis at −1·50 V of a deoxygenated solution of 0·1M TEAP in DMF (79 ml), down to a current smaller than 0·2 mA, 0·108 g of *I* were added to the cathodic compartment of the cell. Then potential was fixed at −1·24 V and purified CO_2 was bubbled through the solution instead of nitrogen. This potential was selected in order to avoid reduction of either CO_2 or 2-bromobenzoic acid, eventually formed as a product. Although this potential corresponds to the rising portion of the polarographic wave, it was negative enough to achieve electrolysis of *I* in a reasonable period of time. It is noteworthy that bubbling of CO_2 did not change the initial current flowing across the cell (c. 30 mA). After 4 hours current dropped to 0·3 mA. The integration of the *I* vs *t* plot gave a transferred charge of 1·85 ± 0·05 electrons/molecule, in striking contrast with polarography and CV results, but in agreement with the values of current and time previously published[5] which indicate an overall charge transfer of about 2 electrons/molecule.

Catholyte (10 ml) was dissolved in water (45 ml) and extracted with hexane (3 × 25 ml). The UV spectrum of this solution revealed peaks at 254 and 260 nm. Solvent was then removed at reduced pressure and residue was dissolved again in hexane. A second UV spectrum revelaed the same absorption bands and new peaks at 267 and 228 nm. Benzene was not found in contrast with the results obtained using this technique in electrolysis of monohalobenzenes[8]. Therefore benzene yield, if any, was less than 1%. We have to note that there are no papers reporting benzene formation from electrolysis of *I*, although this assumption was made by Wawzonek and Wagenknecht[5].

The remaining DMF solution was evaporated under vacuum. The residue was extracted with ether (2 × 5 ml), then acidified with 0·1M-HCl (10 ml) and extracted again with ether (3 × 10 ml). Both organic layers were combined and concentrated to a final volume of 10 ml. A sample was analysed by GC coupled with mass spectrometry. Molecular peaks of 151, 210, 255, 278 and 390 atomic units were obtained, but no products containing either Br or Hg were found. The molecular peak at 210 corresponds to 1,2-diphenyl-1,2-ethanedione, identified by its mass spectrum and its retention time in GC. This product has an adsorption maximum at 260 nm, matching one of the peaks observed in UV spectra. Another sample was analysed by NMR, showing a complex mixture with no acid hydrogens.

These results are in agreement with those obtained from electrolysis of 1-bromo-2-iodobenzene in DMF/TEAP, which produced benzene and bromobenzene amounting to only 9% of the theoretical quantity[12]. Coulometry showed that only 2 electrons

were consumed per molecule. Sease has ascribed these anomalies to formation of benzyne as intermediate[12]. The low number of electrons/molecule indicates that benzyne, removed from Hg surface by mechanical stirring, can disappear by pathways that do not consume electrons and do not yield benzene as the main product. The biradical character of *III* could account for alternative reactions. *III* can be attacked by nucleophiles. In this way electrolysis of 1-bromo-2-iodobenzene in DMF with LiCl yielded chlorobenzene (13%) (ref.[12]). On the other hand, *III* can form dimers or polymers. Diphenylene and triphenylene have been found among products of reaction of 1-bromo-2-fluorobenzene with lithium amalgam in ether, where *III* is formed as intermediate[13]. Triphenylene has also been found in a preparation of *III* (ref.[14]).

However these results did not allow us to draw any conclusions about whether the reduction mechanism of *I* involves a synchronous abstraction of both bromides or not. So we tried to study it from a theoretical point of view. The problem was first approached by computing dianion of *I* (*IV*), since splitting of two C—Br bonds must be preceded by transfer of two electrons. The results obtained are reported in Table IV. Dianion *IV* has an almost symmetrical structure, with most of the charge on the Br atoms. New electrons are in sigma antibonding orbitals and bond orders are quite low. C—Br bonds are stretched, bond angles are opened as a result of repulsion between both Br atoms and there is a certain dihedral angle between them (Table IV), so that there is no symmetry plane in the molecule. In fact each Br atom is on a different side of the aromatic ring. Bending out of the plane is low in order to allow some delocalizatin of electrons in the aromatic ring. This unstable structure has a high heat of formation (94 Kcal mol^{-1}) as compared with *I*.

S^2 value (1·64) shows that *IV* has a singlet state heavily contaminated by triplet state. Nevertheless this value remains almost constant throughout the reaction coordinates, thus contamination becomes irrelevant in the analysis of the results obtained.

For the synchronous pathway, i.e. the one-step abstraction of both bromide ions, the energy profile along the C—Br length of both bonds is shown in Fig. 1 (curve S). Transition state (TS) corresponds to a C—Br distance of c. 2·7 Å, with a minimum energy barrier of 11·2 Kcal mol^{-1}. At this stage charges in Br atoms are about 90% of the total charges, and bond angles are substantially opened. Afterwards the energy decreases quickly.

Asynchronous pathway, the two-step mechanism, is shown in Fig. 1 (curve A). In this case the first TS occurs at a C—Br distance near 2·6 Å and the energy barrier is about 3 Kcal mol^{-1}. The results obtained are shown in Table IV. Afterwards the energy decreases quickly. At a C—Br distance of 3·4 Å the Br charge and bond order indicate that both fragments are practically independent from a chemical point of view. At this point we removed the bromide and the rest of the molecule was optimizated, leading to biradical anion *o*-bromophenyl (*V*), equivalent to *II* in principle;

TABLE IV

Geometrical and electrical parameters computed for several dibromobenzene derivatives in the first step of the bonds fission

Compound	R_{C-Br} Å	Bond order	q_{Br1} [a]	q_{Br2} [a]	q_{C1} [a]	Bond [c] angle	Bending [b] angle
$Br_2C_6H_4^{\cdot-}$	1·90	0·525	−0·32	−0·28	−0·07	122·2	0·1
$Br_2C_6H_4^{2-}$	2·10	0·227	−0·65	−0·65	−0·09	128·6	4·0
			Synchronous path for the dianion				
	2·2	0·206	−0·69	−0·69	−0·07	129·5	4·2
	2·4	0·162	−0·78	−0·78	−0·04	133·2	6·4
	2·6	0·106	−0·86	−0·86	0·00	138·6	10·8
	2·8	0·057	−0·93	−0·93	0·01	141·2	15·7
	3·0	0·024	−0·97	−0·97	0·02	150·0	18·4
			Asynchronous path for the dianion. First step				
	2·2	0·203	−0·70	−0·64	−0·07	129·5	8·8
	2·3	0·180	−0·75	−0·62	−0·05	128·6	35·7
	2·4	0·150	−0·80	−0·61	−0·03	129·6	40·8
	2·6	0·087	−0·89	−0·59	0·00	134·2	42·0
	2·8	0·037	−0·96	−0·59	0·00	138·6	42·8
	3·0	0·014	−0·98	−0·58	−0·02	142·8	43·4
	3·2	0·005	−0·99	−0·58	−0·03	146·7	47·5
	3·4	0·001	−1·00	−0·57	−0·05	150·8	49·6
			Asynchronous path for the monoanion. First step				
$Br_2C_6H_4^{\cdot-}$	2·1	0·260	−0·55	−0·12	−0·11	123·9	1·2
	2·3	0·231	−0·62	−0·09	−0·09	123·9	0·1
	2·5	0·197	−0·70	−0·05	−0·08	124·4	−0·3
	2·7	0·146	−0·80	−0·01	−0·06	125·6	−0·3
	2·9	0·086	−0·89	0·02	−0·04	129·8	1·0
	3·1	0·039	−0·95	0·04	−0·03	136·8	0·6
	3·3	0·013	−0·98	0·04	−0·03	145·9	−0·6
	3·5	0·005	−0·99	0·03	−0·03	145·9	−0·6
	3·7	0·000	−0·99	0·01	−0·04	162·4	−31·3
	3·9	0·000	−0·99	−0·02	−0·04	170·8	−39·3
	4·1	0·000	−0·99	−0·04	−0·05	179·8	−46·1
	4·3	0·000	−0·99	−0·05	−0·05	172·0	−33·3

[a] In atomic units; [b] dihedral angle $Br_1C_1C_2Br_2$; [c] $Br_1C_1C_2$.

but in this case the negative charge is not on the C_1 atom. Instead it is preferentially located on the remaining C—Br bond. This feature allows to understand the reduced basic and nucleophilic character of the intermediate, so that it cannot be trapped by either H^+ or CO_2. Heat of formation of *V* is 55·2 Kcal mol^{-1}. Some other properties of this intermediate are summarized in Table V.

Figure 2 shows the energy profile along the first splitting C—Br bond distance for the monoanion radical of *I*. Stretching of this bond is very easy up to 2·1 Å. Afterwards energy increases quickly up to the TS, located near 3·1 Å with an energy barrier of about 24 Kcal mol^{-1}. Other results are summarized in Table IV. It can be observed that in the TS bond order between both atoms is very low, 95% of the charge resides on the Br and the bond angle is substantially opened. At a C—Br distance of 3·7 Å both fragments are practically independent as can be seen in Table IV. The following step of this asynchronous mechanism is a second electron transfer to the aromatic rest leading to the intermediate *V*.

Figure 3 shows the energy profile along the splitting C—Br bond distance as reaction coordinate for the second step of asynchronous abstraction mechanism. To allow comparison with Fig. 1, the energy of free bromide anion (−37·5 Kcal . . mol^{-1}) has been added, leading to the system energy plotted in Fig. 3. Some further results upon the reaction coordinate are summarized in Table V. TS is located near 3·3 Å with an energy barrier of 28 Kcal mol^{-1}. However this TS is lower than those shown in Fig. 1, due to stability of anion intermediate *V* plus free bromide ion relative to dianion *IV*. As can be seen in Table V, C—Br bond fission is very advanced in the TS.

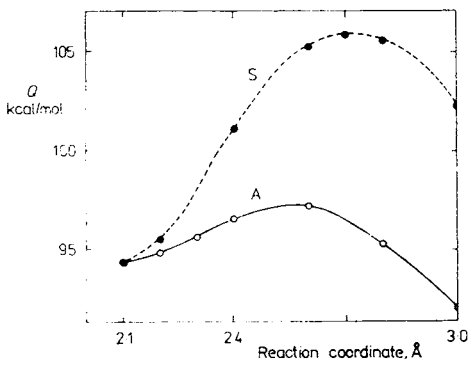

FIG. 1

Energy profiles for the dianion of 1,2-dibromobenzene (*IV*) along the C–Br bond as reaction coordinate. S Synchronous pathway. A Asynchronous pathway, first step

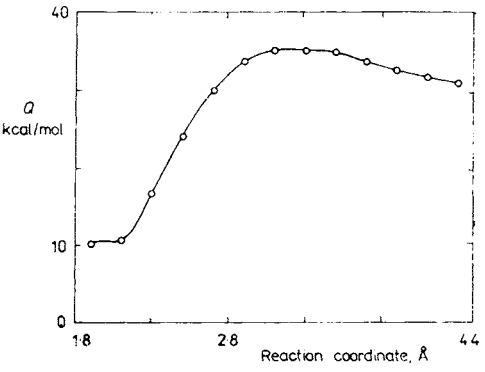

FIG. 2

Energy profile for the monoanion of 1,2-dibromobenzene along the C–Br bond as reaction coordinate

From this theoretical study, we can conclude that stepwise abstraction mechanism is favoured against concerted mechanism. Furthermore, as it would be expected, this results point out that the monoanion radical pathway is easier than the dianion one, since this compound has a much higher heat of formation.

All the reported results are fulfilled by the following mechanism:

$$C_6H_4Br_2 + e \rightleftarrows C_6H_4Br_2^{\dot{-}} \qquad (1)$$

$$C_6H_4Br_2^{\dot{-}} \rightarrow C_6H_4Br^{\bullet} + Br^- \qquad (2)$$

$$C_6H_4Br^{\bullet} + e \rightleftarrows C_6H_4Br^- \ (V) \qquad (3)$$

$$C_6H_4Br^- \rightarrow C_6H_4 \ (III) + Br^- , \qquad (4)$$

where (*1*) must be the r.d.s. since step (*2*) is very fast. In addition step (*3*) has to be fast at the applied potentials since *o*-bromophenyl radical will be easier to reduce than *I* (otherwise both electron transfers would be observed as different waves) and probably easier to reduce than phenyl radical, whose reduction is fast at the applied potential[9]. Further evidence of charge transfer control is displacement of

TABLE V

Geometrical and electrical parameters computed for the intermediate *V* of dibromobenzene reduction in second step of the asynchronous bonds fission

$R_{C_2-Br_2}$	Bond order	q^a_{Br2}	q^a_{C1}	q^a_{C2}	Bond[b] angle
1·97	0·366	−0·49	−0·08	−0·23	132·5
		Asynchronous path. Second step			
2·1	0·293	−0·56	−0·09	−0·17	123·1
2·3	0·243	−0·63	−0·07	−0·14	123·2
2·6	0·173	−0·76	−0·02	−0·11	122·6
2·7	0·144	−0·81	0·00	−0·10	123·0
2·8	0·114	−0·86	0·02	−0·10	124·2
2·9	0·085	−0·90	0·03	−0·09	125·7
3·0	0·060	−0·93	0·04	−0·09	128·4
3·1	0·039	−0·96	0·04	−0·10	133·5
3·2	0·023	−0·97	0·04	−0·10	137·3
3·3	0·015	−0·98	0·03	−0·09	138·7
3·4	0·007	−0·99	0·02	−0·10	148·1

[a] In atomic units; [b] $Br_2C_2C_1$.

$E_{1/2}$ about 100 mV to negative values when using tetrabutylammonium instead of tetraethylammonium as supporting cation. Note that the charge transfer control along with the αn values reported above suggest that n (the number of electrons transfered in the r.d.s.) is 1, like in the reductions of bromobenzene and 1,3-dibromobenzene, and not 2 as required in the mechanism proposed by Wawzonek and Wagenknecht[5] or any other concerted mechanism. The slow decrease of current function with increasing sweep rate (Table II) is consistent with an ECE mechanism where the standard potential for the second electron transfer is less negative than for the first electron transfer[15].

Further evolution after benzyne formation depends on techniques used. In electrolysis, *III* can react chemically as described above. In microelectrochemical techniques, *III* is further reduced since it is electroactive at the applied reduction potential of *I*:

$$III + e \rightleftarrows C_6H_4^{\cdot -} \tag{5}$$

$$C_6H_4^{\cdot -} + H^+ \rightarrow C_6H_5^{\cdot} \tag{6}$$

$$C_6H_5^{\cdot} + e \rightleftarrows C_6H_5^- \tag{7}$$

$$C_6H_5^- + H^+ \rightarrow C_6H_6 . \tag{8}$$

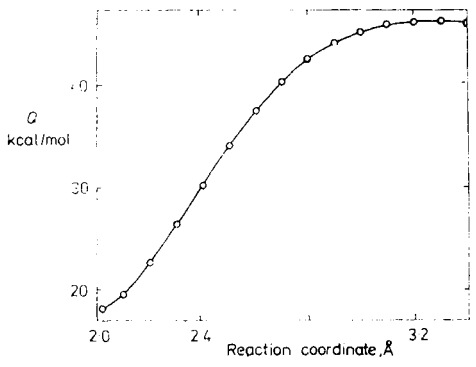

FIG. 3

Energy profile for the biradical anion *o*-bromophenyl (*V*) along the second C–Br bond as reaction coordinate. Second step of the asynchronous pathway

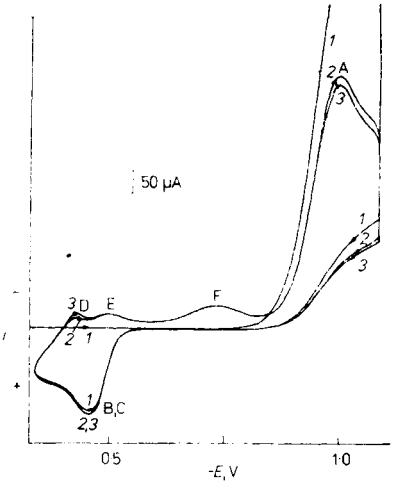

FIG. 4

Cyclic voltammogram of $5 \cdot 10^{-3}$M 1,2-dibromobenzene (*I*) in DMF/0·1M TEAP at 0·3 V s^{-1}. Ordinal numbers of sweeps are given. Anodic currents are labeled +

Presence of proton donors is important in this sequence, thus the wave height increases upon addition of phenol.

CV of 5 . 10^{-3}M solutions of *I* (Fig. 4) shows a set of secondary peaks with a very similar behaviour to those observed in reduction of monohalobenzenes, diphenylmercury and phenylmercury salts[9]. On the other hand, behaviour of *I* at the RRDE is like that of bromobenzene and iodobenzene[9]. An anodic wave appears at the ring electrode (Fig. 5), but only if substrate is being reduced at the disk and if electrode is rotating. Quantitative results are given in Table III. These secondary peaks and waves are due to electrode intermediates and they disappear in presence of added phenol, as observed in monohalobenzene reductions[9]. Therefore, they could also be due to processes:

$$C_6H_5^- - e \rightleftarrows C_6H_5^\bullet \qquad (9)$$

$$C_6H_5^\bullet + Hg \rightleftarrows C_6H_5Hg^\bullet \qquad (10)$$

$$C_6H_5Hg^\bullet - e \rightleftarrows C_6H_5Hg^+ \qquad (11)$$

which could account for anodic waves. Afterwards cathodic waves appear in CV and at the RRDE (Fig. 5). These peaks can be assigned[9] to the reduction:

$$C_6H_5Hg^+ + e \rightleftarrows C_6H_5Hg^\bullet . \qquad (12)$$

Phenylmercury anion could, in turn, support further reactions as explained earlier[9]. One of them:

$$C_6H_5Hg^\bullet + e \rightarrow C_6H_5^- + Hg \qquad (13)$$

accounts for peak F observed by CV.

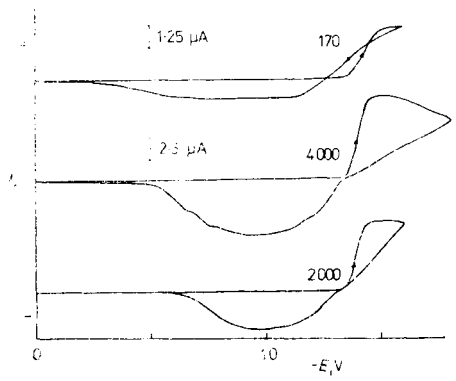

FIG. 5

Ring current vs disk potentials at the RRDE for 1 . 10^{-3}M 1,2-dibromobenzene in DMF/0·1M TEAP. Rotation speeds in rpm are given in the figure. Sweep rate 0·02 V s^{-1}

While the present work was being carried out, a paper was published by Lund et al.[16], whose results fully support the mechanism here proposed. The authors obtained addition products of *o*-bromophenyl radical and anthracene in the reduction of *I* by the photoexcited radical anion of anthraquinone. The minimum concentration of the reductant and the bimolecular character of this homogeneous electron transfer allowed resolution of steps (*1*) and (*3*), and, consequently, trapping of the radical intermediate. Surprisingly this work imputes to Wawzonek and Wagenknecht a different mechanism than that originally proposed by them[5] (Scheme 1).

Thanks to Prof. Juan Bertran for helpful discussions, and to Prof. Desmond A. Bermingham and Montse Julia for help in manuscript correction. This work has been partially supported by a grant of the Ministerio de Educacion y Ciencia, Spain.

REFERENCES

1. Rifi M. R. in: *Organic Electrochemistry* (M. M. Baizer, Ed.), p.294. Marcel Dekker, New York 1973.
2. Fry A. J.: *Synthetic Organic Electrochemistry*, Cap. V. Harper & Row, New York 1972.
3. Závada J., Krupička J., Sicher J.: Collect. Czech. Chem. Commun. *28*, 1664 (1965).
4. Jura W. H., Gaul R. J.: J. Am. Chem. Soc. *80*, 5402 (1958).
5. Wawzonek S., Wagenknecht J. H.: J. Electrochem. Soc. *110*, 420 (1963).
6. Barba F., Guirado A., Zapata A.: Electrochim. Acta *27*, 1335 (1982).
7. Casado J., Gallardo I., Moreno M.: J. Electroanal. Chem. *219*, 197 (1987).
8. Casado J., Gallardo I.: Electrochim. Acta *32*, 1145 (1987).
9. Casado J., Gallardo I.: Collect. Czech. Chem. Commun *54*, 900 (1989).
10. Casado J., Domenech J., Gallardo I.: Monatsh. Chem. *115*, 1143 (1984).
11. Marcus R. A.: J. Chem. Phys.: *24*, 966 (1956); ibid. *43*, 679 (1965).
12. Ref.[2], p. 184.
13. Wittig C., Pohmer L.: Chem. Ber. *89*, 1334 (1956).
14. Luttringhaus A., Schubert K.: Naturwissenschaften *42*, 17 (1955).
15. Nicholson R. S., Shain I.: Anal. Chem. *37*, 178 (1965).
16. Nellebord P., Lund H., Eriksen J.: Tetrahedron Lett. *26*, 1773 (1985).